

Lawrence Berkeley National Laboratory

Recent Work

Title

HYPERFINE-STRUCTURE SEPARATIONS AND NUCLEAR MOMENTS OF GALLIUM-68

Permalink

<https://escholarship.org/uc/item/50x300gt>

Authors

Ehlers, Vernon J.
Shugart, Howard A.

Publication Date

1961-12-18

University of California
Ernest O. Lawrence
Radiation Laboratory

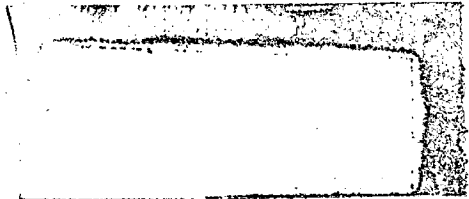
TWO-WEEK LOAN COPY

*This is a Library Circulating Copy
which may be borrowed for two weeks.
For a personal retention copy, call
Tech. Info. Division, Ext. 5545*

Berkeley, California

DISCLAIMER

This document was prepared as an account of work sponsored by the United States Government. While this document is believed to contain correct information, neither the United States Government nor any agency thereof, nor the Regents of the University of California, nor any of their employees, makes any warranty, express or implied, or assumes any legal responsibility for the accuracy, completeness, or usefulness of any information, apparatus, product, or process disclosed, or represents that its use would not infringe privately owned rights. Reference herein to any specific commercial product, process, or service by its trade name, trademark, manufacturer, or otherwise, does not necessarily constitute or imply its endorsement, recommendation, or favoring by the United States Government or any agency thereof, or the Regents of the University of California. The views and opinions of authors expressed herein do not necessarily state or reflect those of the United States Government or any agency thereof or the Regents of the University of California.



UCRL-9991

UNIVERSITY OF CALIFORNIA
Lawrence Radiation Laboratory
Berkeley, California

Contract No. W-7405-eng-48

HYPERFINE-STRUCTURE SEPARATIONS AND NUCLEAR MOMENTS
OF GALLIUM-68

Vernon J. Ehlers and Howard A. Shugart

December 18, 1961

HYPERFINE-STRUCTURE SEPARATIONS AND NUCLEAR MOMENTS
OF GALLIUM-68

Vernon J. Ehlers and Howard A. Shugart

Department of Physics and Lawrence Radiation Laboratory
University of California, Berkeley, California

December 18, 1961

ABSTRACT

The atomic-beam magnetic-resonance method has been used to determine the hyperfine-structure interaction constants of 68-minute Ga^{68} . Measurements performed in both the ${}^2\text{P}_{1/2}$ electronic ground state and the ${}^2\text{P}_{3/2}$ first excited state give the results

$${}^2\text{P}_{1/2}: |a| = 11.716 \pm 0.010 \text{ Mc/sec,}$$

$${}^2\text{P}_{3/2}: |a| = 1.660 \pm 0.010 \text{ Mc/sec,}$$

$$|b| = 10.276 \pm 0.017 \text{ Mc/sec,}$$

$$b/a < 0.$$

The small value of the magnetic dipole interaction constant results in an inversion of the hyperfine-structure energy levels in the ${}^2\text{P}_{3/2}$ state. In descending order, the levels for an assumed positive moment diagram are $F = 3/2, 5/2,$ and $1/2$.

The uncorrected nuclear moments calculated from these measurements and from known constants of the stable gallium isotopes are

$$|\mu_I| = 0.01172 \pm 0.00006 \text{ nm,}$$

$$|Q| = 0.0313 \pm 0.0016 \text{ b.}$$

The stated uncertainty in the magnetic moment is large enough to include the effect of a possible hyperfine-structure anomaly. The dipole and quadrupole moments have opposite signs.

HYPERFINE-STRUCTURE SEPARATIONS AND NUCLEAR MOMENTS
OF GALLIUM-68*Vernon J. Ehlers[†] and Howard A. ShugartDepartment of Physics and Lawrence Radiation Laboratory
University of California, Berkeley, California

December 18, 1961

INTRODUCTION

The nuclear spin of Ga⁶⁸ was determined with the atomic beam method by Hubbs, Marrus, and Worcester, who also observed evidences of small hyperfine-structure separations.¹ Since a preliminary assignment of resonances indicated the existence of an extremely small nuclear magnetic moment and an inversion of the hyperfine-structure energy levels,² it was of interest to continue the measurements. Although initial investigations appeared to confirm the preliminary level assignment,³ further investigation revealed that resonances which had been assigned to $\Delta F = 0$ transitions were in fact direct ($\Delta F = \pm 1$) transitions, and that the original level assignment was in error. Because of the small hyperfine-structure separations it was found necessary to adopt a different resonance search and identification procedure. Subsequent measurements described here determined the correct level order and resonance assignments and yielded the hyperfine-structure separations in the $^2P_{1/2}$ and $^2P_{3/2}$ electronic states.

THEORY

The hyperfine-structure Hamiltonian for a free atom in an external magnetic field H is

$$\mathcal{H} = ha \mathbf{L} \cdot \mathbf{J} + hb \frac{3(\mathbf{L} \cdot \mathbf{J})^2 + (3/2) \mathbf{L} \cdot \mathbf{J} - I(I+1)J(J+1)}{2I(2I-1)J(2J-1)} - g_J \mu_0 \mathbf{J} \cdot \mathbf{H} - g_I \mu_0 \mathbf{I} \cdot \mathbf{H},$$

where a and b are the hyperfine-structure magnetic-dipole and electric-quadrupole interaction constants, respectively, I and J are the nuclear and electronic angular momenta in units of \hbar , and μ_0 is the absolute value of the Bohr magneton. The electronic and nuclear g factors are defined by $g_J = \mu_J/J$ and $g_I = \mu_I/I$, where both magnetic moments are expressed in Bohr magnetons.

For $J = 1/2$ no quadrupole interaction exists and the secular equation of this Hamiltonian can be solved analytically.⁴ For $J > 1/2$ the problem is most conveniently solved by a numerical method. For both cases, the energy eigenvalues and transition frequencies were obtained by using electronic digital computers. Plotting the energy of the atomic system as a function of magnetic field, we obtain the familiar energy-level diagram. Figures 1 and 2 show these diagrams for the $^2P_{1/2}$ and $^2P_{3/2}$ states of Ga^{68} , as calculated from the final observed values of the interaction constants, assuming a positive magnetic moment. Because of the small hyperfine-structure separations, the Paschen-Back region begins to dominate at very low magnetic fields.

In order to correlate the experimental data with the hyperfine-structure Hamiltonian, another computer program was used to fit any combination of the four parameters a , b , g_J , and g_I to the observed data by minimizing the function⁵

$$N(a, b, g_J, g_I) = \sum_i R_i^2 \omega_i.$$

The value of this function at minimum is the χ^2 of the fit. The residual, R_i , of the i th observation is given by

$$R_i = f_i - W_i(F_1, m_1) + W_i(F_2, m_2),$$

where f_i is the observed resonance frequency and the $W_i(F, m)$ are the calculated energies of the levels between which the transition occurred. The weight factor ω_i is defined by

$$\omega_i = \frac{1}{(\delta f_i)^2 + \left(\frac{\partial f_i}{\partial H} \delta H_i\right)^2},$$

where δf_i and δH_i are the uncertainties in the observed frequency and magnetic field, respectively. The derivative $\frac{\partial f_i}{\partial H}$ is calculated by the program.

After trial values of the parameters to be varied are initially given, the routine proceeds to search for the minimum of the function N , and improves the values of the parameters with each iteration.

Because the nuclear moments and interaction constants of the stable gallium isotopes are known,^{6, 7, 8, 9} it is possible to obtain the nuclear moments of Ga^{68} from the observed interaction constants by using the relations

$$\left(\frac{g_I}{a}\right)_{\text{Ga}^{68}} = \left(\frac{g_I}{a}\right)_{\text{Ga}^{69}},$$

$$\left(\frac{Q}{b}\right)_{\text{Ga}^{68}} = \left(\frac{Q}{b}\right)_{\text{Ga}^{69}}.$$

The derivation of these equations involves the assumption of a point nucleus. Deviations from these equations are caused by the difference in spatial distribution of nuclear magnetism and charge in the two isotopes involved. This effect is called the hyperfine-structure anomaly.¹⁰ It is expected to be very small for P states, and in fact is less than $10^{-2}\%$ for the stable gallium isotopes. With high enough precision, measurement of the interaction constants of an isotope in two electronic states allows the determination of the hyperfine-

structure anomaly without a direct measurement of the magnetic moment.¹¹ Unfortunately, here the uncertainties in the Ga^{68} results allow us to do no more than place an upper limit on the size of the anomaly.

ISOTOPE PRODUCTION AND PREPARATION

The Berkeley 60-inch cyclotron was used to produce the Ga^{68} radioisotope by the reaction $\text{Cu}^{65}(\alpha, n)\text{Ga}^{68}$. A 10-mil sheet copper target was mounted on the internal probe of the cyclotron, where much greater beam currents are available than in the external beam. The maximum beam current used was $120\mu\text{a}$, and targets typically received a total bombardment of $70\ \mu\text{a-hr}$ during a bombardment of approximately 40 minutes. Several other gallium isotopes were produced simultaneously by various reactions during the bombardments, but only Ga^{66} was present in sufficient quantity to interfere with the Ga^{68} measurements. The large amount of Ga^{66} present made it mandatory to complete the experiment as rapidly as possible, before the Ga^{68} signal disappeared into the Ga^{66} background. Also, when searching for Ga^{68} resonances, it was necessary to avoid regions containing Ga^{66} resonances.

The chemical separation by ether extraction of the radioactive gallium from the target copper has been described earlier.¹ Various improvements in technique increased the yield without increasing the time required for separation. Typical separations of better than 75% were achieved, and in general less than 80 minutes elapsed between removal of the target from the cyclotron and exposure of the first samples in the atomic-beam machine. Because of the extreme radioactivity of the samples all chemical separations were performed inside a 2-inch lead-enclosed cave.

EXPERIMENTAL METHOD

Standard techniques of radioactive atomic-beam work¹² were used throughout this experiment, with the exception of the search procedure outlined below. The magnetic field was calibrated by observing the Rb⁸⁵ and Rb⁸⁷ $\Delta F=0$ transitions. Very good beams of gallium atoms were obtained by using graphite ovens, but slow variations of beam intensity were observed. Although the two electronic states of gallium are almost equally populated at the 1300°C operating temperature of the oven, the atomic-beam apparatus used in this experiment favors the isotope of larger g_J . As a result, the $^2P_{3/2}$ resonances observed were approximately three times as high as those of the $^2P_{1/2}$ state. A $^2P_{1/2}$ transition or a $^2P_{3/2}$ transition with a low transition probability could be observed only during the early part of an experimental run, whereas a $^2P_{3/2}$ transition possessing a large transition probability could be seen as late as 2 hours after the start of a run.

During a typical experimental run lasting 2 hours, approximately 20 samples were exposed. These samples were counted in continuous-flow methane counters immediately after removal from the atomic-beam machine, and thus rough resonance curves were obtained during the run itself. Usually about 14 samples per run would be meaningful, so these samples were counted a number of times sufficient to establish a good decay curve. Each decay curve was analyzed into components by a least-squares technique which yielded the relative amount of Ga⁶⁸ present on each sample at an arbitrary zero time. The counting rate of each sample was normalized by the half-beam method¹³ to compensate for the variations in beam intensity. The ratio method¹³ of normalization is also possible in this case because of the presence of the Ga⁶⁶, but the percentage uncertainty of the Ga⁶⁶ counting rates on the samples was large enough to make this method less accurate than the half-beam method.

The search procedure used in this experiment differs slightly from standard techniques. Ordinarily, one observes the $\Delta F=0$ transitions at progressively higher magnetic fields until the hyperfine-structure separations are known well enough to permit a search for the direct $\Delta F=\pm 1$ transitions. Because of the small hfs separations in Ga^{68} , the frequencies of the direct transitions are already of the same order of magnitude as the $\Delta F=0$ transition frequency at the low magnetic field of 10 gauss. Thus the problem is not only one of locating resonances, but also one of identifying those resonances which are observed. The misidentification of several $\Delta F=\pm 1$ resonances as $\Delta F=0$ transitions resulted in the previously reported erroneous level assignment.³ Subsequent investigation indicated the smallness of the interaction constants, and revealed that the reported resonance assignment was only one of a number that fitted the observed data very well. Thus it became evident that a different search and identification procedure was necessary.

One simple procedure would be to set the magnetic field as near to zero as possible and then proceed to search for the direct transitions. Unfortunately it was impossible to set the magnetic field below 3 gauss with the machine used in this research, and thus this procedure was not feasible. An alternative attempt was made to observe the $^2P_{3/2} \Delta m_J = \pm 1, \Delta m_I = 0$ transitions in the extreme Paschen-Back region. In this region we should see three resonances at the frequencies $\nu_0, \nu_0 + a$, and $\nu_0 - a$, where $\nu_0 = -g_J \mu_0 H/h$, and a is the magnetic-dipole interaction constant. Unfortunately Ga^{66} has $I=0$ and therefore also has a resonance at the frequency ν_0 . Figure 3 shows the Ga^{66} and Ga^{68} counting rates of the samples obtained during this high-field search. In addition, this figure demonstrates the success of the method of resolving the counting rate of a sample into its component counting rates. We note the occurrence of the expected Ga^{66}

resonance at ν_0 , and two unresolved Ga^{68} resonances at ν_0 and $\nu_0 + a$. Because the large magnetic-field inhomogeneities at this high field make it impossible to resolve these resonances, no exact value of a in the $^2P_{3/2}$ state could be obtained in this manner. The observation does, however, place an upper limit on a .

The next step was an attempt to determine the $^2P_{1/2}$ interaction constant, in spite of the greater difficulty in observing resonances in this state. Since b is zero for this state, it is necessary to fit only the one parameter a to the observed data, thus simplifying the identification problem. Initial searches for the $\Delta F=0$ transition were conducted at relatively high fields, where there was small likelihood that any $^2P_{3/2}$ resonances were present. The transitions observed allowed the determination of the hyperfine-structure separation $\Delta\nu$ to within a few hundred kc/sec. Then a search for the $\Delta F=\pm 1$ direct transitions yielded several resonances belonging to both electronic states. By means of resonance height and field dependence it was possible to assign definitely several of the resonances to the $^2P_{1/2}$ state, thus giving an accurate value of $\Delta\nu$.

Because the interaction constants of the stable gallium isotopes are known, it was possible to calculate the $^2P_{3/2}$ a from the observed value of a in the $^2P_{1/2}$ state. Thus only b remained to be determined. Even so, there were a number of values of b which fitted the previously observed data. The procedure then adopted was to calculate the resonance frequencies expected for the various possible values of b , and conduct searches for these resonances. Because of wide variations in the observed transition probabilities it was difficult to predict which transitions would be most easily found. Thus at the beginning of a run, a sample was exposed on the peak of each of the expected resonances. Figure 4 shows the result of such a search. Those

resonances which displayed a high counting rate were then observed more carefully, either in the same run or in subsequent runs. Proceeding in this manner it was soon possible to eliminate all but one level assignment. A large number of resonances were taken at varying magnetic fields in order to verify this final assignment.

Some transitions in each electronic state pass through field-independent points, i. e., $\frac{\partial f}{\partial H}$ becomes zero. At these points field inhomogeneities have little effect on the line width, and the observed resonance width should be the natural width caused by the finite transit time of the atom through the radiofrequency region. Figures 5, 6, and 7 show typical resonances obtained at these field-independent points. Their small line width permits the accurate determination of the hyperfine-structure separations. Figure 7 shows the type of resonance frequently observed for a σ transition which is excited by a hairpin designed for π transitions.¹⁴ The characteristic pattern with a minimum at resonance is caused by the atom passing through two successive radiofrequency fields 180° out of phase.

RESULTS

All resonances identified as belonging to the $^2P_{3/2}$ state are listed in Table I. The experimental data are the resonance frequencies of Ga⁶⁸ and of the calibration isotope. The experimental uncertainty in the last place of each quantity is given in parentheses following that quantity. Each resonance is assigned to a transition $(F_1, m_1) \leftrightarrow (F_2, m_2)$, based on an assumed positive moment diagram. The result of a least-squares fit to the data is given, and the residual for each resonance is also listed. Note that in every case the residual is smaller than the uncertainty of the resonance frequency. The various atomic and nuclear constants of the calibrating and comparing isotopes used in the least-squares calculation are also listed. The $^2P_{1/2}$ data are

given in a similar manner in Table II. It should be mentioned that the resonances of this state assigned to the $(3/2, 1/2) \longleftrightarrow (1/2, -1/2)$ transition belong as well to the $(3/2, -1/2) \longleftrightarrow (1/2, 1/2)$ transition, since these transitions have nearly the same resonance frequencies at low fields.

A large number of resonances were obtained before the level order was firmly established, and thus some turned out to be unresolved superpositions of two resonances. All such unresolved resonances are listed in Table III; also given are the transitions that have been assigned to them. The frequencies of these transitions at the observed fields have been calculated from the final values of the interaction constants.

The fit of the final values of the interaction constants to the observed low-field data is demonstrated graphically in Figures 8, 9, and 10. Each point on the graphs represents an observed resonance, while the lines show the calculated transition frequencies as a function of magnetic field. The identification of each resonance shown in Figs. 8 and 9 is given in Table IV. Unless shown otherwise, the experimental uncertainty of each point is smaller than the size of that point. Figure 8 shows the ${}^2P_{1/2}$ data, Fig. 9 the ${}^2P_{3/2}$ data, and Fig. 10 all the observed data, including the unresolved resonances. The final values of the interaction constants provide an excellent fit to all the observed data.

In Table I a number of resonances have been assigned to $\Delta F = \pm 2$ transitions. These transitions are usually not expected, since they violate the low-field selection rule, which requires $\Delta F = 0, \pm 1$. However, because of the small hyperfine-structure separations, at approximately 4 gauss we are already in the intermediate-field region where F is no longer a good quantum number. In particular, the $(5/2, 1/2) \longleftrightarrow (1/2, 1/2)$ transition is a good example of this. Even though it disobeys both the high-field and low-

field selection rules, it is readily observable between 3 and 15 gauss, and, in fact, has a resonance height greater than the $(3/2, -1/2) \leftrightarrow (1/2, 1/2)$ transition, which is allowed at both high and low fields. The existence and size of these resonances added greatly to the difficulty in determining a consistent assignment.

Tables I and II give the results of a least-squares fit to the data listed there. The χ^2 is small for both electronic states, especially for the $^2P_{1/2}$ data. This indicates a very good fit to the observed data, and a high probability that the actual values of a and b lie within the limits of error given by the program. Nevertheless, the limits are increased to include the possibility of a systematic error. Thus we obtain for the final values of the $^2P_{3/2}$ hyperfine-structure interaction constants

$$|a| = 1.660 \pm 0.010 \text{ Mc/sec,}$$

$$|b| = 10.276 \pm 0.017 \text{ Mc/sec,}$$

$$b/a < 0,$$

and for the $^2P_{1/2}$ state

$$|a| = 11.716 \pm 0.010 \text{ Mc/sec.}$$

From these values we obtain the following hyperfine-structure separations for an assumed positive moment:

$$^2P_{3/2} \quad \Delta\nu_{5/2, 3/2} = -8.695 \pm 0.033 \text{ Mc/sec,}$$

$$\Delta\nu_{3/2, 1/2} = 25.611 \pm 0.041 \text{ Mc/sec,}$$

$$^2P_{1/2} \quad \Delta\nu_{3/2, 1/2} = 17.574 \pm 0.015 \text{ Mc/sec.}$$

Calculated from a Fermi-Segrè type relation, the uncorrected electric quadrupole moment is

$$|Q| = 0.0313 \pm 0.0016 \text{ b,}$$

and the uncorrected magnetic dipole moments as calculated from the interaction constants of the two electronic states are

$${}^2P_{1/2}: |\mu_I| = 0.011729 \pm 0.000010 \text{ nm},$$

$${}^2P_{3/2}: |\mu_I| = 0.01166 \pm 0.00007 \text{ nm}.$$

The stated uncertainty of Q is due entirely to the uncertainty in the quadrupole moment of the stable isotope used in the calculation. The uncertainties quoted for the magnetic moments are due only to the uncertainties of the interaction constants and thus do not include the possible effect of a hyperfine-structure anomaly. Because the measurements were performed in two electronic states we are able to set an upper limit to the size of the anomaly. For the ${}^2P_{1/2}$ state we obtain that the anomaly is less than 0.6%. The anomaly is usually smaller than this for P states, but on the basis of our results we can assign only this upper limit with certainty.

If we assume that the difference between the two calculated magnetic moments is entirely due to experimental uncertainty, we must take the weighted average of the two. Doing this, and assigning 0.6% uncertainty to include the effect of a possible hyperfine-structure anomaly, we obtain, for the uncorrected nuclear magnetic dipole moment,

$$|\mu_I|_{\text{uncorr}} = 0.01172 \pm 0.00006 \text{ nm}.$$

Applying the diamagnetic correction¹⁵ $K = 1.00262$, we obtain for the corrected moment

$$|\mu_I|_{\text{corr}} = 0.01175 \pm 0.00006 \text{ nm}.$$

Because the value of b/a is negative, the nuclear dipole and quadrupole moments have opposite signs.

DISCUSSION OF RESULTS

Calculations of the magnetic moment expected on the basis of the single-particle model give $\mu_I = -0.94$ nm if the theoretical g factors are used, and $\mu_I = -0.35$ nm if the empirical g values of the neighboring odd-proton and odd-neutron nuclei are used.¹⁶ The observed magnetic moment of $\mu_I = \pm 0.01$ is much smaller than either of the calculated values.

It would be interesting to continue these measurements for two reasons. First, although the small magnitude of the magnetic moment precludes the possibility of determining its sign by the usual method of determining whether a positive or negative moment clearly gives the best least-squares fit to the data (the so-called χ^2 test), it is possible to measure the sign of the moment directly by using the method of Childs, Goodman, and Kieffer.¹⁷ Secondly, more accurate measurements of the interaction constants would determine whether the difference in the moments calculated from the results of the two states is due to a hyperfine-structure anomaly, or is merely an experimental discrepancy.

ACKNOWLEDGMENTS

We would like to thank Dr. John L. Worcester for supplying us with the data he had obtained on this isotope, and also for stimulating our interest in this problem. We would also like to thank the crew of the Crocker 60-inch cyclotron for their proficient handling of the extremely radioactive targets, Mrs. Ruth-Mary Larimer for her careful attention in monitoring the radiochemical handling, and Mr. Michael De Vito for his competent assistance in counting the samples.

REFERENCES

*Supported in part by the U. S. Atomic Energy Commission and the U. S. Office of Naval Research.

† Presently on leave as a NATO Postdoctoral Fellow at Erstes Physikalisches Institut der Universität Heidelberg, Germany.

1. J. C. Hubbs, R. Marrus, and J. L. Worcester, Phys. Rev. 110, 534 (1958).
2. J. L. Worcester, private communication (1959).
3. V. J. Ehlers and W. A. Nierenberg, Bull. Am. Phys. Soc. II, 4, 452 (1959).
4. G. Breit and I. I. Rabi, Phys. Rev. 38, 2082 (1931).
5. Hugh L. Garvin, Thomas M. Green, Edgar Lipworth, and William A. Nierenberg, Phys. Rev. 116, 393 (1959).
6. R. T. Daly, Jr. and J. H. Holloway, Phys. Rev. 96, 539 (1954).
7. A. Lurio and A. G. Prodell, Phys. Rev. 101, 79 (1956).
8. M. Rice and R. V. Pound, Phys. Rev. 99, 1036 (1955).
9. G. F. Koster, Phys. Rev. 86, 148 (1952).
10. A. Bohr and V. F. Weisskopf, Phys. Rev. 77, 94 (1950); H. H. Stroke, R. J. Blin-Stoyle, and V. Jaccarino, Phys. Rev. 123, 1326 (1961).
11. T. G. Eck, A. Lurio, and P. Kusch, Phys. Rev. 106, 954 (1957).
12. For example, see W. A. Nierenberg, Ann. Rev. Nuclear Sci. 7, 349 (1957).
13. V. J. Ehlers, W. A. Nierenberg, and H. A. Shugart, (submitted to Phys. Rev.)
14. W. J. Childs, L. S. Goodman, and L. J. Kieffer, Phys. Rev. 122, 891 (1961).

15. W. C. Dickinson, Phys. Rev. 80, 563 (1950).
16. M. H. Brennan and A. M. Bernstein, Phys. Rev. 120, 927 (1960).
17. W. J. Childs, L. S. Goodman, and L. J. Kieffer, Phys. Rev. 120, 2138 (1960).

Table I. Summary of Ga⁶⁸ 2P_{3/2} data

Run	Calibration frequency ^a (Mc/sec)	Magnetic field ^d (gauss)	Ga ⁶⁸ frequency (Mc/sec)	F ₁	m ₁	F ₂	m ₂	Residual (kc/sec)
1 ^b	0.500(25) ^c	0.711(35)	0.800(50)	5/2	1/2	5/2	-1/2	+2
2 ^b	1.000(25) ^c	1.418(35)	1.630(60)	5/2	1/2	5/2	-1/2	+30
3 ^b	2.000(25) ^c	2.819(35)	3.250(100)	5/2	1/2	5/2	-1/2	+8
4 ^b	3.010(25) ^c	4.215(34)	5.030(50)	5/2	1/2	5/2	-1/2	+28
5 ^b	1.000(25) ^c	1.418(35)	2.145(50)	3/2	-1/2	3/2	-3/2	-21
6 ^b	1.500(25) ^c	2.121(35)	3.370(50)	3/2	-1/2	3/2	-3/2	+6
7 ^b	2.000(25) ^c	2.819(35)	4.635(65)	3/2	-1/2	3/2	-3/2	+34
252	2.994(40)	6.383(85)	8.225(125)	5/2	1/2	5/2	-1/2	+93
4911	6.147(25)	13.037(52)	18.800(200)	5/2	1/2	1/2	1/2	-32
5033	3.284(25)	6.998(53)	9.025(150)	5/2	1/2	5/2	-1/2	-100
5431	5.419(30)	11.507(63)	16.600(200)	5/2	1/2	1/2	1/2	+45
5611	1.448(30)	3.095(64)	17.375(75)	5/2	3/2	1/2	1/2	+20
574	2.593(25)	5.531(53)	12.085(30)	5/2	1/2	1/2	1/2	-12
5771	3.762(20)	8.010(42)	14.000(175)	3/2	-1/2	3/2	-3/2	-93
5772	3.762(20)	8.010(42)	12.700(75)	5/2	1/2	1/2	1/2	-13
5773	3.762(20)	8.010(42)	10.875(175)	5/2	1/2	5/2	-1/2	+20
5871	3.142(20)	6.697(42)	21.180(30)	3/2	-1/2	1/2	1/2	-7
5872	3.142(20)	6.697(42)	19.335(40)	5/2	3/2	1/2	1/2	-13
5961	1.656(25)	3.538(53)	21.060(125)	3/2	-1/2	1/2	1/2	+24
5962	1.656(25)	3.538(53)	13.200(200)	5/2	1/2	1/2	1/2	-2
602	2.575(20)	5.493(42)	20.755(20)	3/2	-1/2	1/2	1/2	+6
6061	2.328(25)	4.968(53)	20.697(13)	3/2	-1/2	1/2	1/2	-2
6062	2.811(20)	5.994(42)	12.045(25)	5/2	1/2	1/2	1/2	+5
6181	2.837(25)	6.049(53)	12.055(25)	5/2	1/2	1/2	1/2	+16
6311	2.301(25)	4.911(53)	14.450(250)	3/2	-1/2	5/2	-1/2	+103
6312	2.309(25)	4.928(53)	12.225(150)	5/2	1/2	1/2	1/2	-66
6381	2.108(25)	4.500(53)	12.475(50)	5/2	1/2	1/2	1/2	-32
6382	2.113(25)	4.511(53)	12.460(60)	5/2	1/2	1/2	1/2	-41
6411	1.413(30)	3.020(64)	17.375(40)	5/2	3/2	1/2	1/2	+38
6451	1.538(30)	3.287(64)	35.850(500)	3/2	1/2	1/2	-1/2	+85
6452	2.445(25)	5.217(53)	12.145(40)	5/2	1/2	1/2	1/2	-36
6481	1.643(35)	3.510(75)	11.950(200)	3/2	-1/2	5/2	-1/2	+32
6482	1.643(35)	3.510(75)	13.200(150)	5/2	1/2	1/2	1/2	-26

- a. Calibration in terms of the Rb⁸⁵(3, -2) ↔ (3, -3) transition, unless otherwise indicated.
- b. Data supplied by J. L. Worcester.
- c. Calibration in terms of the K³⁹(2, -1) ↔ (2, -2) transition.
- d. Calculated from the calibration frequency.

Result of least-squares fit: a = ±1.660 ± 0.004 Mc/sec, b = ± 10.276 ± 0.007 Mc/sec;

χ² = 4.9 for 33 observations.

Comparing isotope	Calibration isotopes	
Ga ⁷¹ , 2P _{3/2} , I = 3/2	K ³⁹ , 2S _{1/2} , I = 3/2	Rb ⁸⁵ , 2S _{1/2} , I = 5/2
g _J = - 1.333941	g _J = - 2.002309	g _J = - 2.002409
g _I = + 9.2765 × 10 ⁻⁴	g _I = + 1.41945 × 10 ⁻⁴	g _I = + 2.93704 × 10 ⁻⁴
a = + 242.433949 Mc/sec	Δν = + 461.7197 Mc/sec	Δν = + 3035.735 Mc/sec

Table II. Summary of Ga⁶⁸ $^2P_{1/2}$ data.

Run	Calibration frequency ^a (Mc/sec)	Magnetic field ^b (gauss)	Ga ⁶⁸ frequency (Mc/sec)	F ₁	m ₁	F ₂	m ₂	Residual (kc/sec)
5601	5.408(25)	11.484(53)	5.175(60)	3/2	-1/2	3/2	-3/2	-20
5602	11.908(30)	25.021(62)	14.930(100)	3/2	-1/2	3/2	-3/2	+22
5612	1.448(30)	3.095(64)	17.800(125)	3/2	1/2	1/2	-1/2	+16
5613	1.448(30)	3.095(64)	18.700(100)	3/2	1/2	1/2	1/2	-34
564	1.459(30)	3.118(64)	16.825(25)	3/2	-1/2	1/2	-1/2	-5
5671	2.108(30)	4.500(64)	16.655(20)	3/2	-1/2	1/2	-1/2	+3
5672	3.054(20)	6.510(42)	16.575(25)	3/2	-1/2	1/2	-1/2	+5
569	2.574(25)	5.491(53)	16.584(15)	3/2	-1/2	1/2	-1/2	-2
5831	3.061(25)	6.525(53)	22.050(100)	3/2	3/2	1/2	1/2	+12
5832	3.061(25)	6.525(53)	20.450(250)	3/2	1/2	1/2	1/2	+28
5833	3.061(25)	6.525(53)	18.500(100)	3/2	1/2	1/2	-1/2	+4
5851	3.762(20)	8.010(42)	18.960(35)	3/2	1/2	1/2	-1/2	+6
5852	3.762(20)	8.010(42)	16.645(50)	3/2	-1/2	1/2	-1/2	-2
5901	50.505(20)	100.003(37)	82.230(100)	3/2	-1/2	3/2	-3/2	-29
5902	50.505(20)	100.003(37)	105.580(125)	3/2	3/2	1/2	1/2	-21
6182	2.837(25)	6.050(53)	16.566(20)	3/2	-1/2	1/2	-1/2	-4
6412	1.413(30)	3.020(64)	17.785(40)	3/2	1/2	1/2	-1/2	+11

a. Calibration in terms of the Rb⁸⁵ (3, -2) \longleftrightarrow (3, -3) transition.

b. Calculated from the calibration frequency.

Result of least-squares fit: $a = +1.716 \pm 0.004$ Mc/sec;

$\chi^2 = 0.63$ for 17 observations.

Comparing isotope	Calibrating isotope
Ga ⁷¹ , $^2P_{1/2}$, I = 3/2	Rb ⁸⁵ , $^2S_{1/2}$, I = 5/2
$g_J = -0.665825$	$g_J = -2.002409$
$g_I = +9.27651 \times 10^{-4}$	$g_I = +2.93704 \times 10^{-4}$
$a = +1701.34729$ Mc/sec	$\Delta\nu = +3035.735$ Mc/sec

Table III. Summary of Ga⁶⁸ unresolved resonances

Run	Calibration frequency ^a (Mc/sec)	Magnetic field ^b (gauss)	Ga ⁶⁸ frequency (Mc/sec)	Electronic state	F ₁	m ₁	F ₂	m ₂	Calcu- lated fre- quency ^c (Mc/sec)
282	4.708(20)	10.008(42)	14.435(150)	$\left\{ \begin{array}{l} {}^2P_{3/2} \\ {}^2P_{3/2} \end{array} \right.$	5/2	1/2	5/2	-1/2	14.542
					5/2	1/2	1/2	1/2	14.606
4912	6.131(25)	13.005(52)	20.775(200)	$\left\{ \begin{array}{l} {}^2P_{3/2} \\ {}^2P_{1/2} \end{array} \right.$	5/2	1/2	5/2	-1/2	20.422
					3/2	1/2	1/2	-1/2	21.081
5032	3.284(25)	6.998(53)	12.225(150)	$\left\{ \begin{array}{l} {}^2P_{3/2} \\ {}^2P_{3/2} \end{array} \right.$	3/2	-1/2	3/2	-3/2	12.236
					5/2	1/2	1/2	1/2	12.193
5432	5.419(30)	11.507(63)	17.400(200)	$\left\{ \begin{array}{l} {}^2P_{3/2} \\ {}^2P_{1/2} \end{array} \right.$	5/2	1/2	5/2	-1/2	17.455
					3/2	-1/2	1/2	-1/2	17.269
5433	5.419(30)	11.507(63)	20.425(150)	$\left\{ \begin{array}{l} {}^2P_{3/2} \\ {}^2P_{1/2} \end{array} \right.$	3/2	-1/2	3/2	-3/2	20.516
					3/2	1/2	1/2	-1/2	20.355
557	5.384(25)	11.433(52)	6.775(75) ^d	$\left\{ \begin{array}{l} {}^2P_{3/2} \\ {}^2P_{1/2} \end{array} \right.$	3/2	-1/2	3/2	-3/2	6.824
					3/2	1/2	1/2	-1/2	6.781

a. Calibration in terms of the Rb⁸⁵ (3, -2) \longleftrightarrow (3, -3) transition.

b. Calculated from the calibration frequency.

c. Calculated using a = 1.660 Mc/sec, b = - 10.276 Mc/sec, and $\Delta\nu=17.574$ Mc/sec.

d. This resonance is a third harmonic of the resonance frequency of the transitions listed, and was observed at a high rf power level. It is not shown in Fig. 10.

Table IV. Key to observed transitions in Figs. 8 and 9.

Designation	${}^2P_{3/2}$ Transition				Designation	${}^2P_{1/2}$ Transition			
	F_1	m_1	F_2	m_2		F_1	m_1	F_2	m_2
a	5/2	1/2	5/2	-1/2	m	3/2	-1/2	3/2	-3/2
b	3/2	-1/2	3/2	+3/2	n	3/2	-1/2	1/2	-1/2
c	3/2	-1/2	5/2	-1/2	o	3/2	1/2	1/2	-1/2
d	5/2	1/2	1/2	1/2				3/2	-1/2
e	5/2	3/2	1/2	1/2	p	3/2	1/2	1/2	1/2
f	3/2	-1/2	1/2	1/2	q	3/2	3/2	1/2	1/2
g	3/2	1/2	1/2	-1/2					

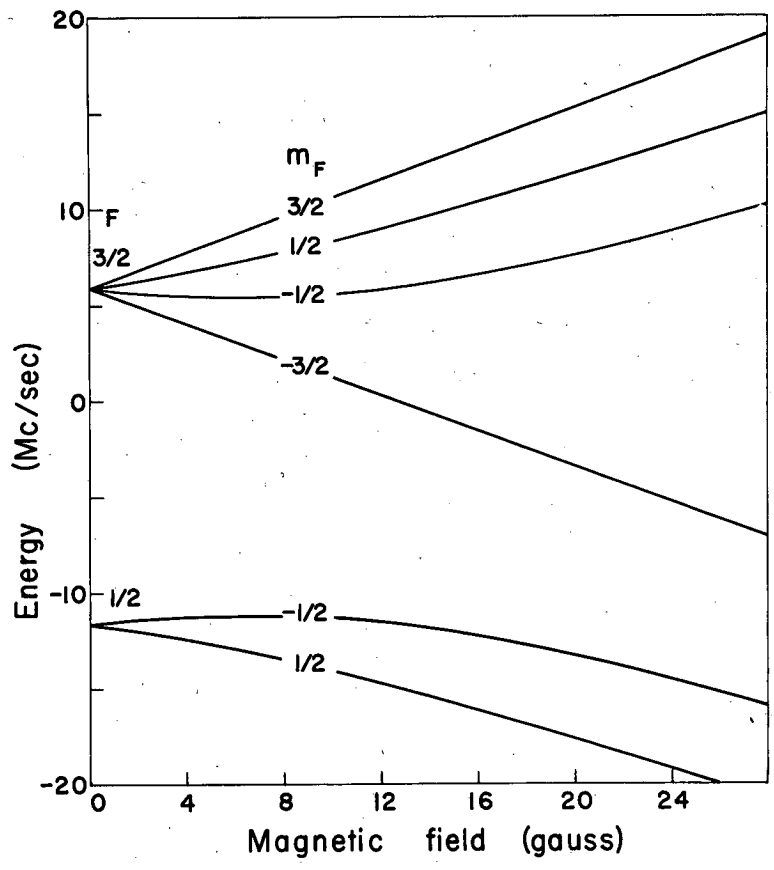
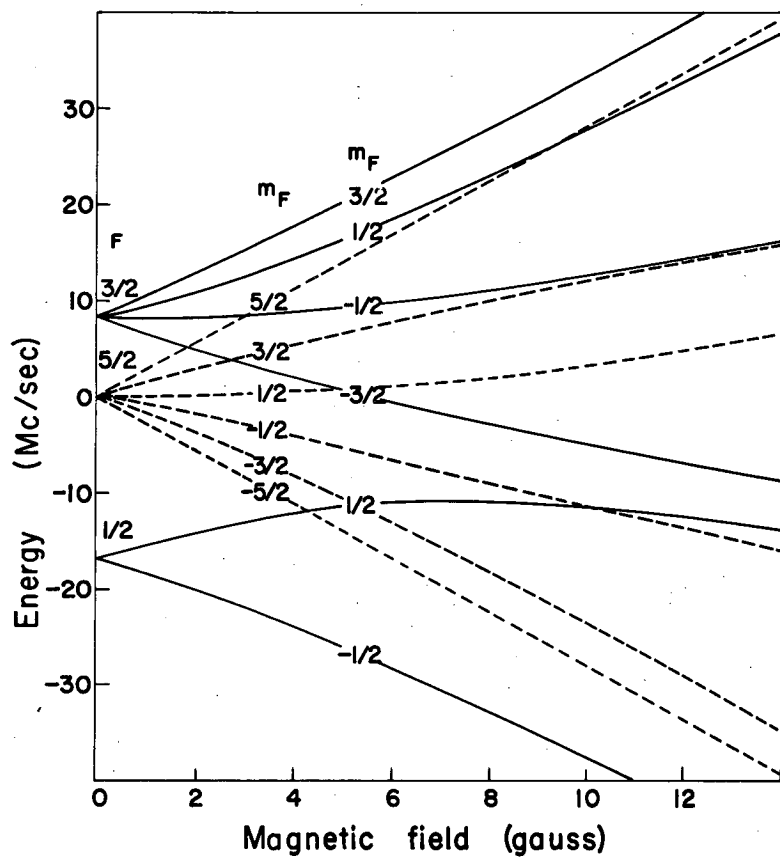
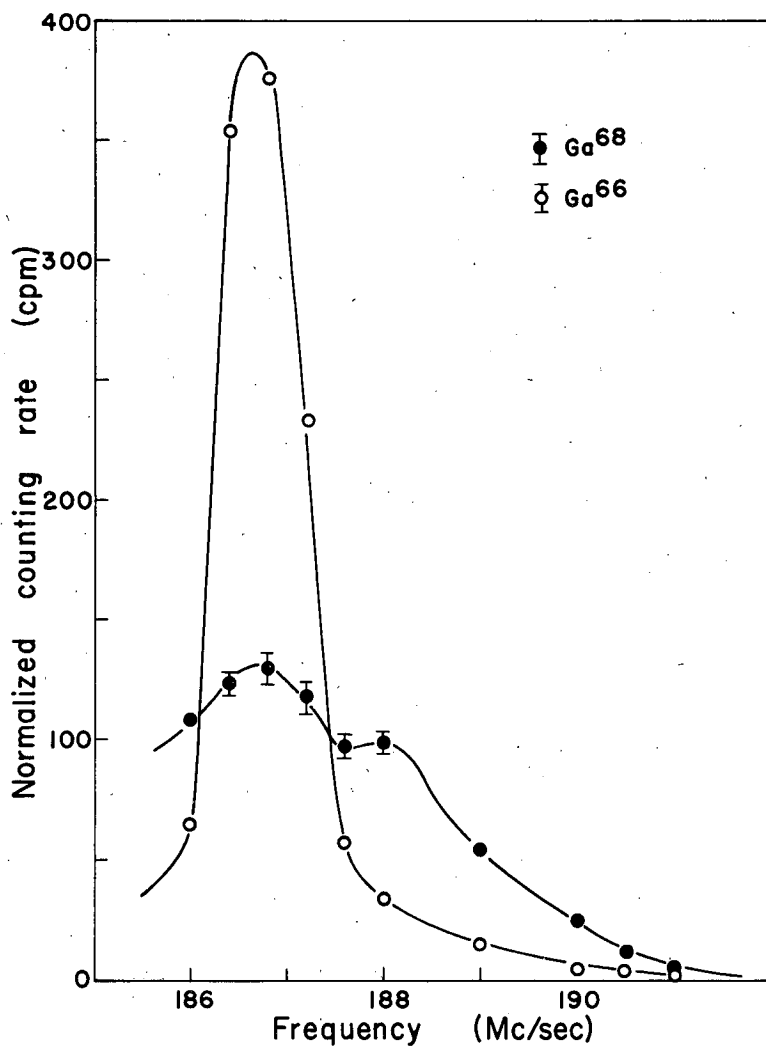


Fig. 1. Breit-Rabi diagram for the $^2P_{1/2}$ electronic state of Ga^{68} (calculated for $\Delta\nu = +17.574$ Mc/sec).



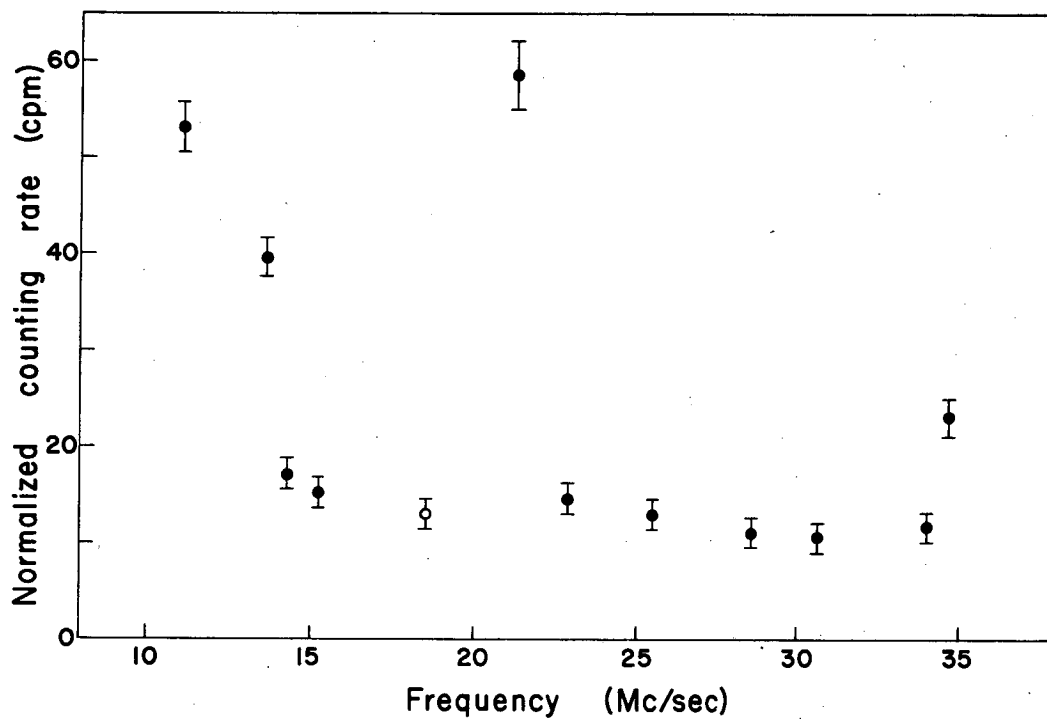
MU-25580

Fig. 2. Breit-Rabi diagram for the $^2P_{3/2}$ electronic state of Ga^{68} (calculated for $a = + 1.660$ Mc/sec, $b = - 10.276$ Mc/sec).



MU-25581

Fig. 3. Ga⁶⁶ and Ga⁶⁸ resonances observed at H = 99.965 gauss.



MU-25582

Fig. 4. A search for possible resonances, conducted at 3.020 gauss. (The open circle point displayed at 18.5 Mc/sec was taken with the rf off.)

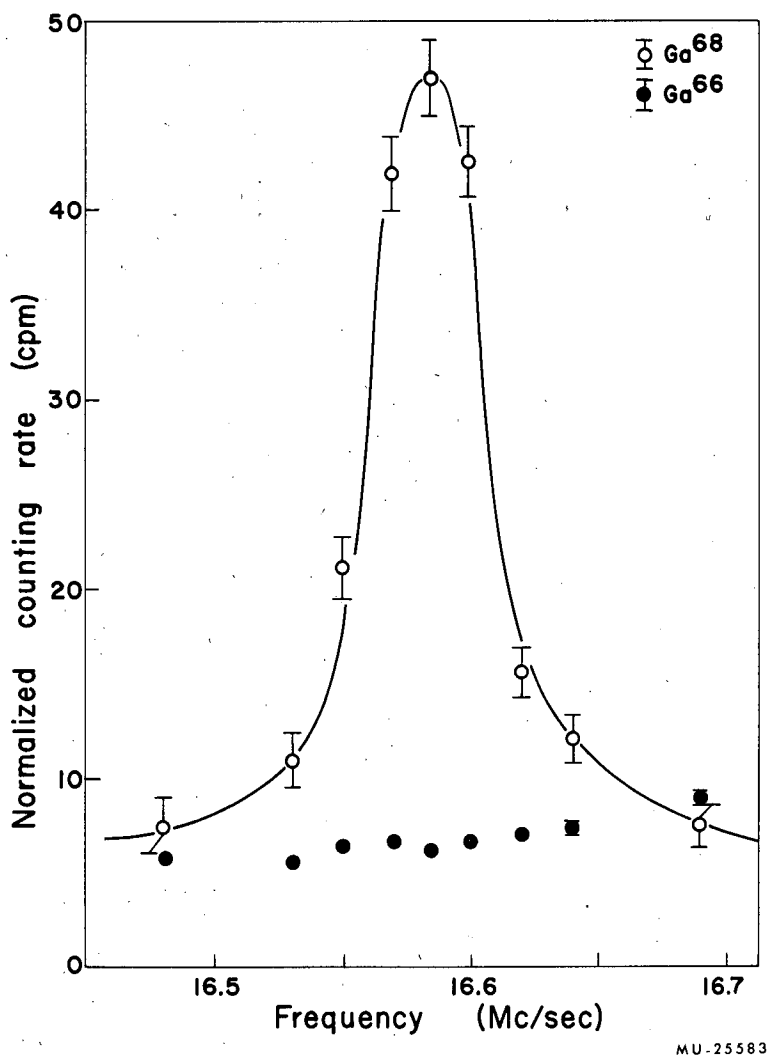
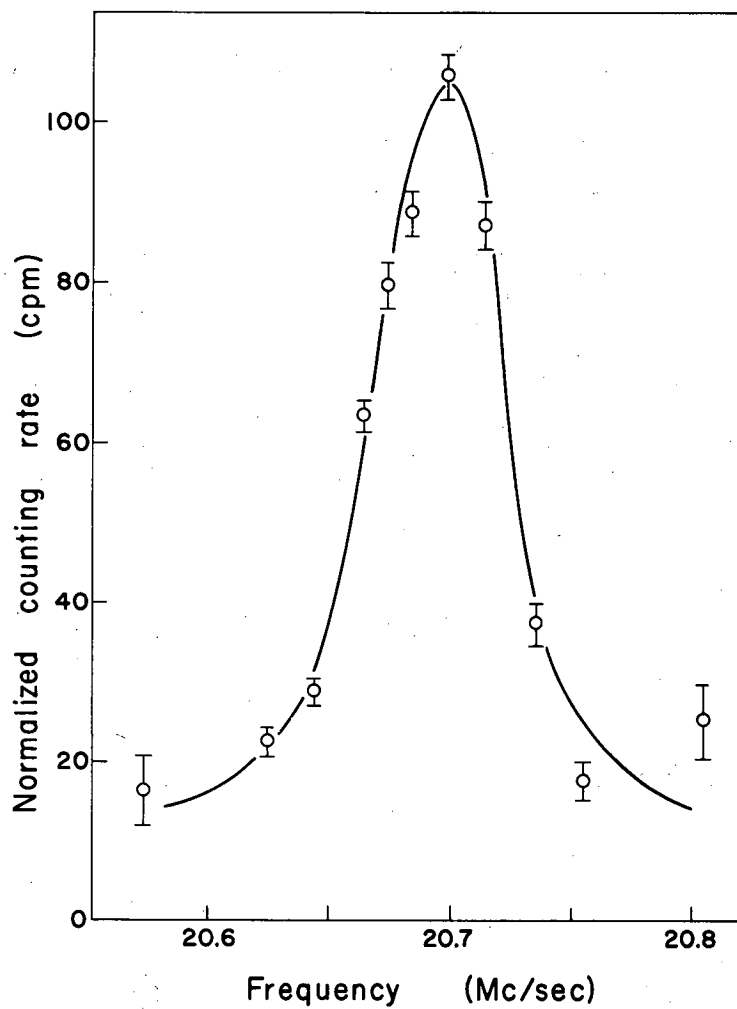


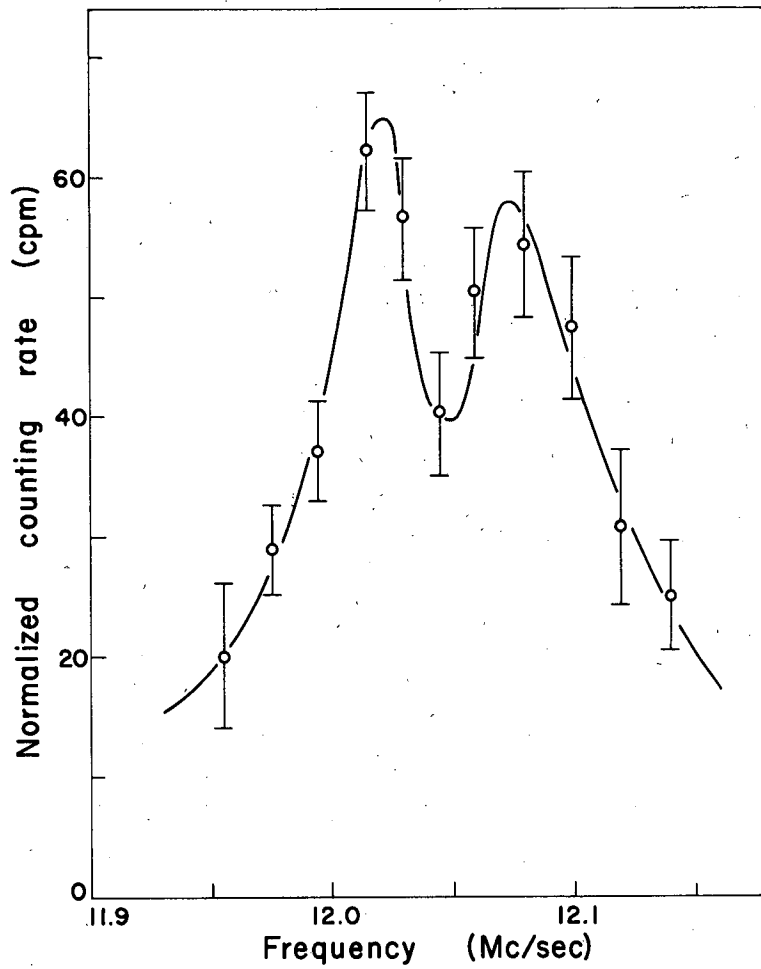
Fig. 5. A resonance corresponding to the transition $(3/2, -1/2) \longleftrightarrow (1/2, -1/2)$ in the $^2P_{1/2}$ electronic state of Ga⁶⁸. (H = 5.491 gauss.) The Ga⁶⁶ background component is also displayed.

MU-25583



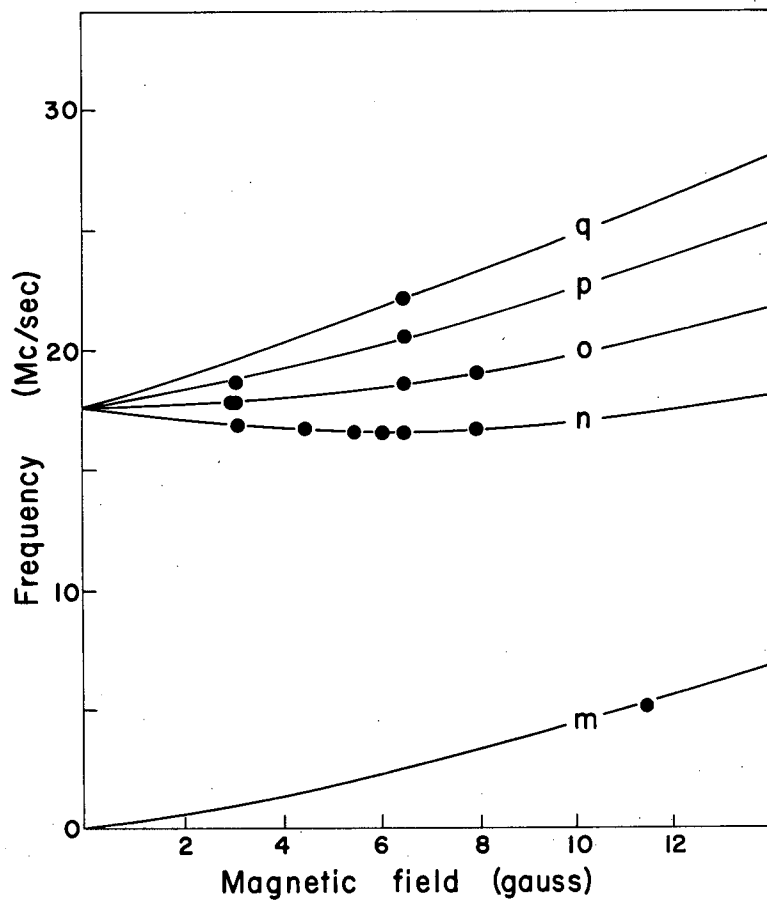
MU-25584

Fig. 6. A resonance corresponding to the $(3/2, -1/2) \leftrightarrow (1/2, 1/2)$ transition in the $^2P_{3/2}$ electronic state of Ga^{68} . ($H = 4.968$ gauss).



MU-25585

Fig. 7. A resonance corresponding to the $(5/2, 1/2) \leftrightarrow (1/2, 1/2)$ transition in the ${}^2P_{3/2}$ electronic state of Ga^{68} . ($H = 5.994$ gauss).



MU-25586

Fig. 8. Comparison with the $^2P_{1/2}$ observed resonances to the theoretical transition frequencies calculated for $\Delta\nu = +17.574$ Mc/sec. Resonance identifications are listed in Table IV.

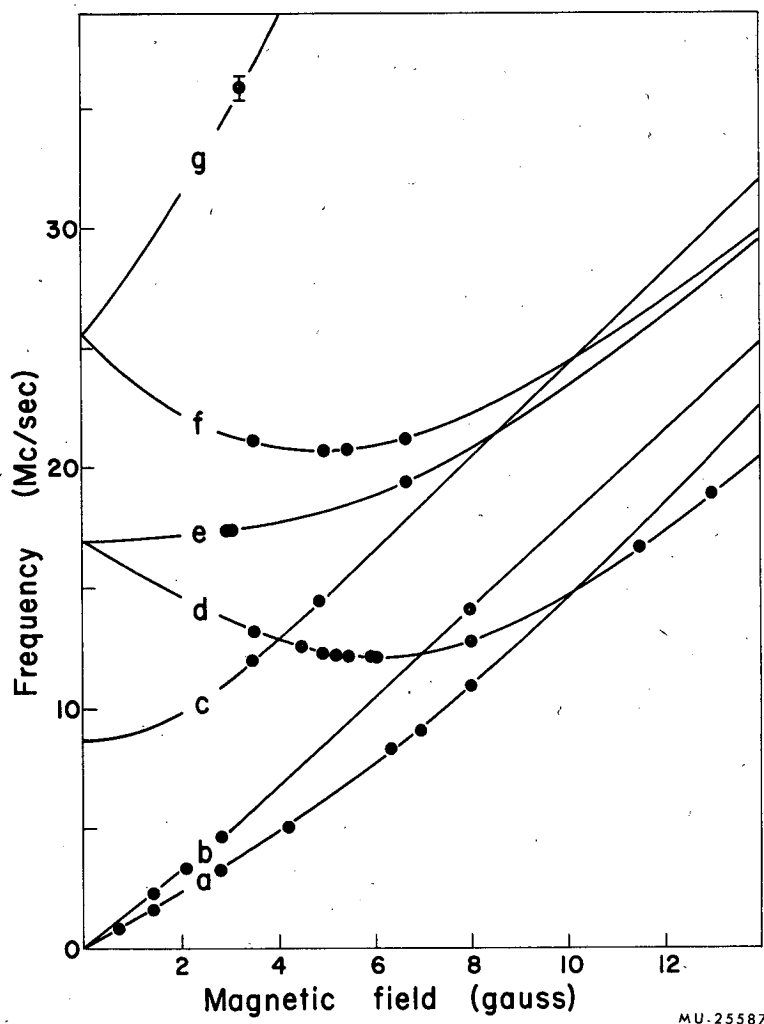
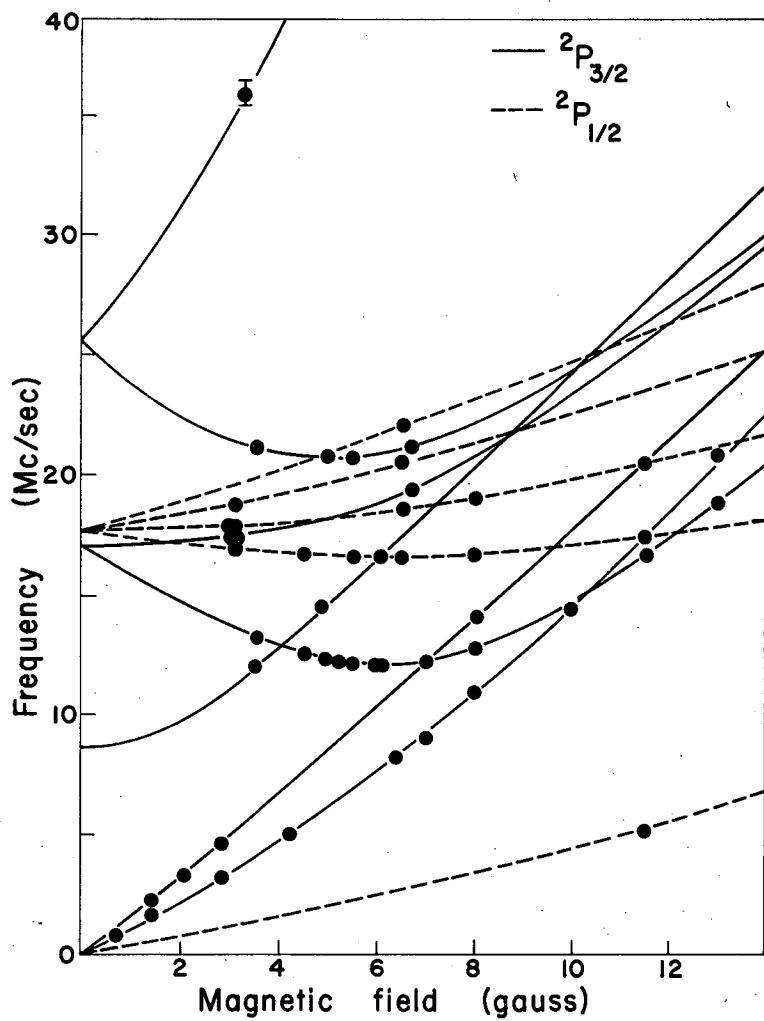


Fig. 9. Comparison with the $^2P_{3/2}$ observed resonances to the theoretical transition frequencies calculated for $a = + 1.660$ Mc/sec, $b = - 10.276$ Mc/sec. Resonance identifications are listed in Table IV.



MU.25588

Fig. 10. Comparison with the observed resonances to the theoretical transition frequencies calculated for $a = + 1.660$ Mc/sec, $b = - 10.276$ Mc/sec, and $\Delta\nu = + 17.574$ Mc/sec. The solid lines represent the $^2P_{3/2}$ electronic state, and the dashed lines the $^2P_{1/2}$ state.

This report was prepared as an account of Government sponsored work. Neither the United States, nor the Commission, nor any person acting on behalf of the Commission:

- A. Makes any warranty or representation, expressed or implied, with respect to the accuracy, completeness, or usefulness of the information contained in this report, or that the use of any information, apparatus, method, or process disclosed in this report may not infringe privately owned rights; or
- B. Assumes any liabilities with respect to the use of, or for damages resulting from the use of any information, apparatus, method, or process disclosed in this report.

As used in the above, "person acting on behalf of the Commission" includes any employee or contractor of the Commission, or employee of such contractor, to the extent that such employee or contractor of the Commission, or employee of such contractor prepares, disseminates, or provides access to, any information pursuant to his employment or contract with the Commission, or his employment with such contractor.